

# Spontaneous growth of 2D coordination polymers on functionalized ferromagnetic surfaces

Michele Mattera,<sup>+</sup> Víctor Rubio-Giménez,<sup>+</sup> Sophie Delprat,<sup>§</sup> Richard Mattana,<sup>§</sup> Pierre Seneor,<sup>§</sup> Sergio Tatay,<sup>\*‡</sup> Alicia Forment-Aliaga,<sup>\*‡</sup> Eugenio Coronado<sup>+</sup>

<b>MATERIALS AND METHODS</b> .....	3
<i>Reagents</i> .....	3
<i>Substrate Preparation</i> .....	3
<i>SAM functionalization and island formation</i> .....	3
<i>Contact Angle (CA) measurements</i> .....	3
<i>Atomic Force Microscopy (AFM)</i> .....	3
<i>Optical microscopy</i> .....	3
<i>Scanning Electron Microscopy (SEM)</i> .....	3
<i>Auger Electron Spectroscopy (AES)</i> .....	4
<i>Raman</i> .....	4
<i>X-Ray diffraction</i> .....	4
<b>SUPPLEMENTARY FIGURES AND TABLES</b> .....	5
Table S1 .....	5
Figure S1 .....	6
Figure S2 .....	7
Figure S3 .....	8
Figure S4 .....	9
Table S2 .....	10
Table S3 .....	10
Table S4 .....	10
Figure S5 .....	11
Table S5 .....	12
Figure S6 .....	12
Figure S7 .....	13
Figure S8 .....	13
Figure S9 .....	14
Figure S10 .....	15
Figure S11 .....	16

## Supporting Information

Figure S12 .....	17
Figure S13 .....	18
Figure S14 .....	18
Figure S15 .....	19

## MATERIALS AND METHODS

**Reagents.** 1-tetradecanethiol (Sigma-Aldrich, 98%) (C14S), 1-hexadecanethiol (Sigma-Aldrich, 99%) (C16S), 1-octadecanethiol (Sigma-Aldrich, 98%) (C18S) and glycolic acid (Sigma-Aldrich, 99%) (GA) are commercially available and were used without any further purification. Absolute Ethanol (HPLC grade) and molecular sieves, 5 Å were bought from Sigma-Aldrich. Syringe Filters with Polypropylene Housing (0.13 mm, 0.2 µm) were bought from VWR.

**Substrate Preparation.** Before FM evaporation, silicon substrates were sonicated  $3 \times 10$  min in freshly prepared  $\text{H}_2\text{O}_2/\text{NH}_4\text{OH}/\text{H}_2\text{O}$  (1:1:2) “basic piranha” solutions, rinsed with milli-Q water, sonicated for 5 min in milli-Q water twice, and dried under a  $\text{N}_2$  stream. Permalloy (Py) layers were deposited onto silicon or glass substrates using a tungsten basket coated Edwards Auto 500 thermal evaporator placed inside a nitrogen glovebox. Base pressure was  $2 \times 10^{-6}$  mbar and evaporation rate 0.02 nm/s. Cobalt (Co) layers were deposited using a Plassys MP9000 sputtering system, under an Ar pressure of  $2.5 \times 10^{-6}$  mbar. The deposition rate is around 0.9 Angstrom/ s. For both surfaces 15 nm was the preferred thickness.

**SAM functionalization and island formation.** A glycolic acid solution (10% in weight in 10 mL) was prepared inside the glovebox, using anhydrous absolute ethanol, previously dried using molecular sieves. An alkanethiol 1 mM ethanolic solution of 10 mL (CnS) was prepared inside the glovebox, using anhydrous absolute ethanol.

The substrates were transferred into the glovebox, dipped into the 2 mL of the filtered GA solution for 15 min, then 2 mL of the filtered CnS solution were added. After 16 hours, the substrates were rinsed with fresh anhydrous absolute ethanol and dried under a  $\text{N}_2$  stream. The substrates were then exposed to air in order to start the island growth.

**Contact Angle (CA) measurements.** Dynamic water contact angle measurements of the samples were performed in air using a Ramé-hart 200 standard goniometer equipped with an automated dispensing system. The initial drop volume was 0.17 µL, increased by additions of 0.08 µL and waiting times of 1500 ms for each step.

**Atomic Force Microscopy (AFM).** The substrates were imaged with a Digital Instruments Veeco Nanoscope IVa AFM microscope in tapping and contact mode. Silicon tips with natural resonance frequency of 300 kHz and with an equivalent constant force of 40 N/m were used. Gwyddion software was used to process the obtained images.

**Optical microscopy.** Optical images were obtained with a NIKON Eclipse LV-100 Optical microscope, equipped with Neutral Density Filters (ND50).

**Scanning Electron Microscopy (SEM).** S-4800 (HITACHI) Scanning electronic microscope with a spotlight of field emission (FEG) and a resolution of 1.4 nm at 1 keV was used. The acceleration voltage used was of 20 keV.

**Auger Electron Spectroscopy (AES).** AES experiments were performed in a PHI 670 Scanning Auger Nanoprobe (Physical Electronics) with a Schottky field emission electron gun as excitation source, Cylindrical Mirror Analyser (CMA) and Multichannel Detector system. In order to avoid inhomogeneity the analyzed area was about 2 microns around the center of reference. Electrons of 10 keV of energy were sent perpendicularly to the surface of the sample and a Fix Retard Ratio mode was used to collect the electrons with an energy step of 1 eV for the whole range. MULTIPAK software has been used to obtain the derivative spectra.

**Raman.** Raman spectra were acquired with a micro-Raman (model XploRA ONE from Horiba, Kyoto, Japan) with a power of 4.5 mW, wavelength 532 nm, grating of 1800 gr/mm, slit of 50  $\mu\text{m}$ , and hole of 100  $\mu\text{m}$ .

**Synchrotron X-Ray diffraction.** X-ray data was collected at the I07 Beamline at Diamond Light Source, Didcot, U.K. (proposal SI14922-1). Samples were placed into a closed cell mounted on a multiaxis diffractometer and measured under a continuous He flow at room temperature. Out-of-plane patterns were acquired in a  $\theta$ - $2\theta$  scattering geometry with a step size of  $0.04^\circ$  using a Pilatus 100K detector with a wavelength of 0.9918  $\text{\AA}$  (beam energy of 14.53 keV).

## SUPPLEMENTARY FIGURES AND TABLES

**Table S1** - Contact angle values measured on the different types of samples used in this work.

Sample	Description	CA(adv/rec) [deg]
 <p>Co-Ox</p>	15 nm of cobalt film evaporated over native silicon oxide and exposed to air for few minutes to carry out contact angle measurements.	35/-
 <p>etch</p>	Cobalt film treated with glycolic acid under inert atmosphere to remove cobalt oxide and exposed to air during contact angle measurements.	10/-
 <p>SAM</p>	C18S SAM grown over a glycolic acid-treated cobalt film under inert atmosphere and exposed to air during contact angle measurements.	114/102
	C18S SAM grown over a glycolic acid-treated cobalt film under inert atmosphere and exposed to air for 16h before contact angle measurements.	100/63

**Figure S1** – a) Schematic representation of lamellar structures growth process: (i) Silicon substrate covered by several nm of a ferromagnetic material with a native oxide layer is placed inside a glovebox. (ii) After chemical etching of the oxide layer a CnS SAM is formed in solution on the recovered surface. (iii) As long as the sample is kept under inert atmosphere a perfect SAM structure is maintained. (iii) Once the sample is taken out from the glovebox and exposed to air, lamellar structures start growing, which get stabilized after approx. 16h. b) and c) Optical images of Co-C18S SAM before (b) and after (c) air exposition. d) and e) AFM topographic images taken under inert atmosphere of a Co-C18S (d) and Py-C18S (e) samples.

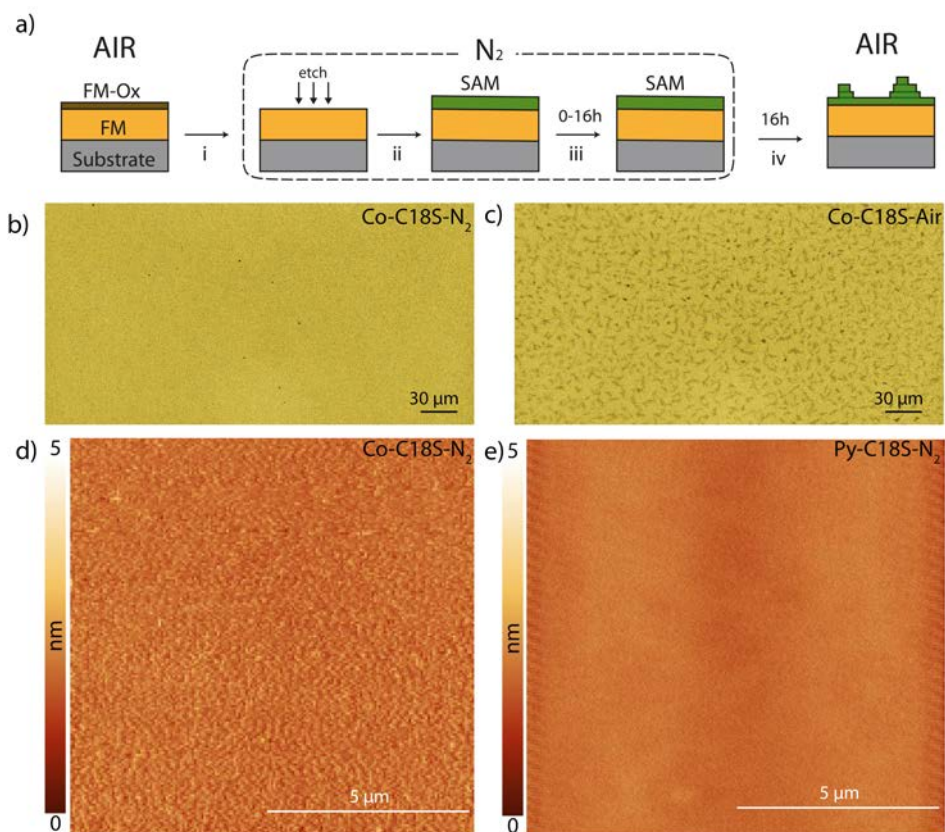
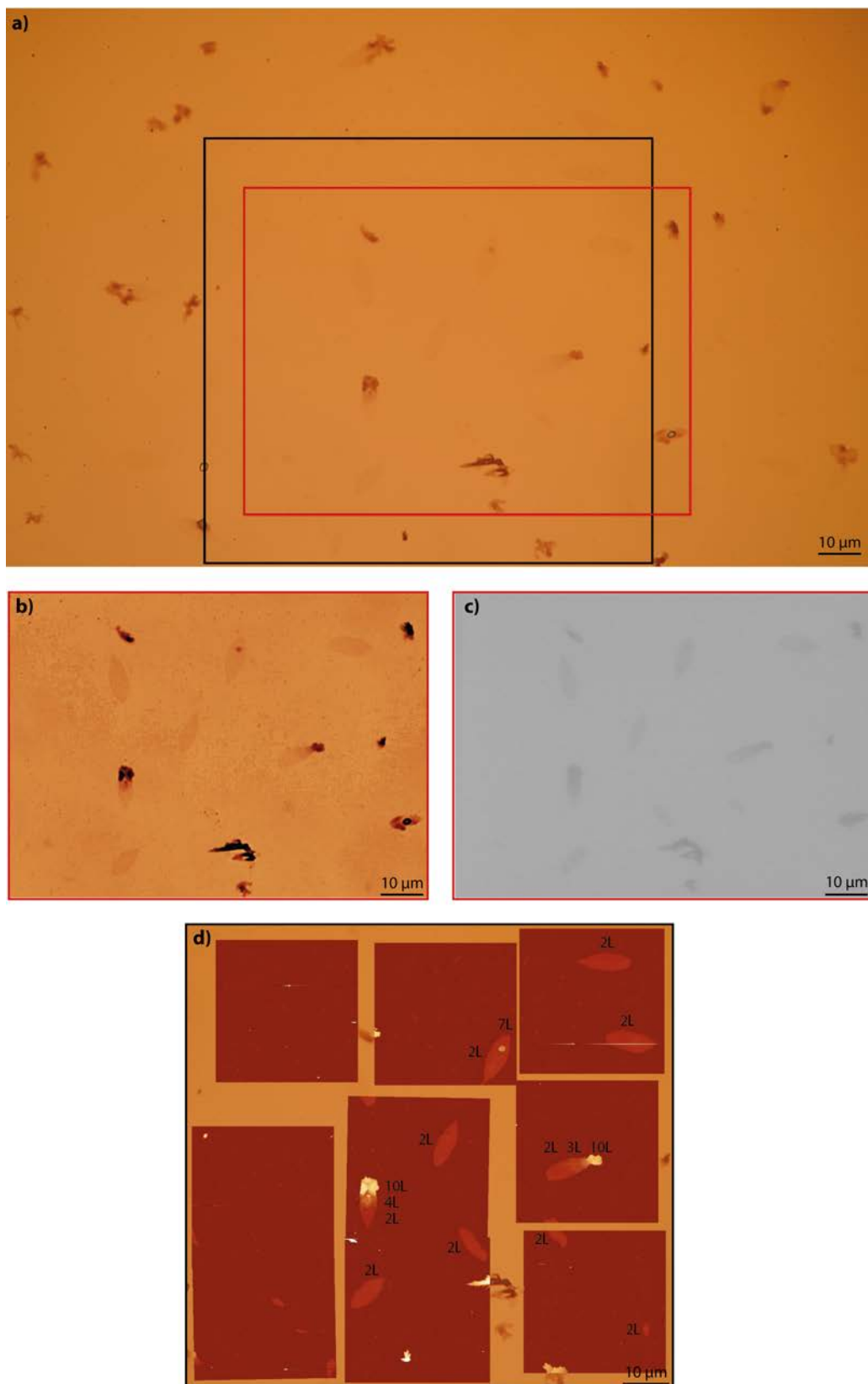
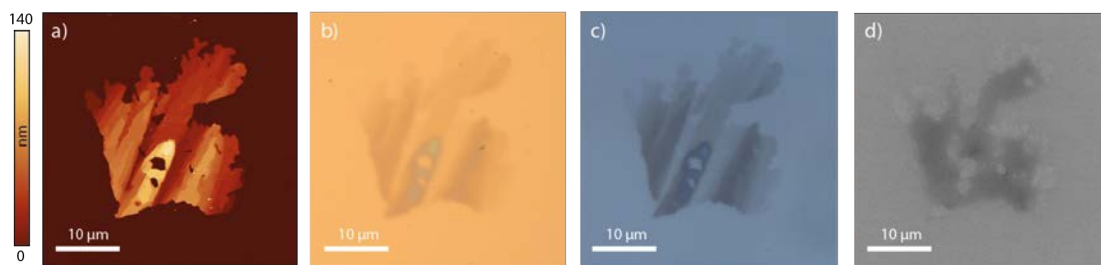


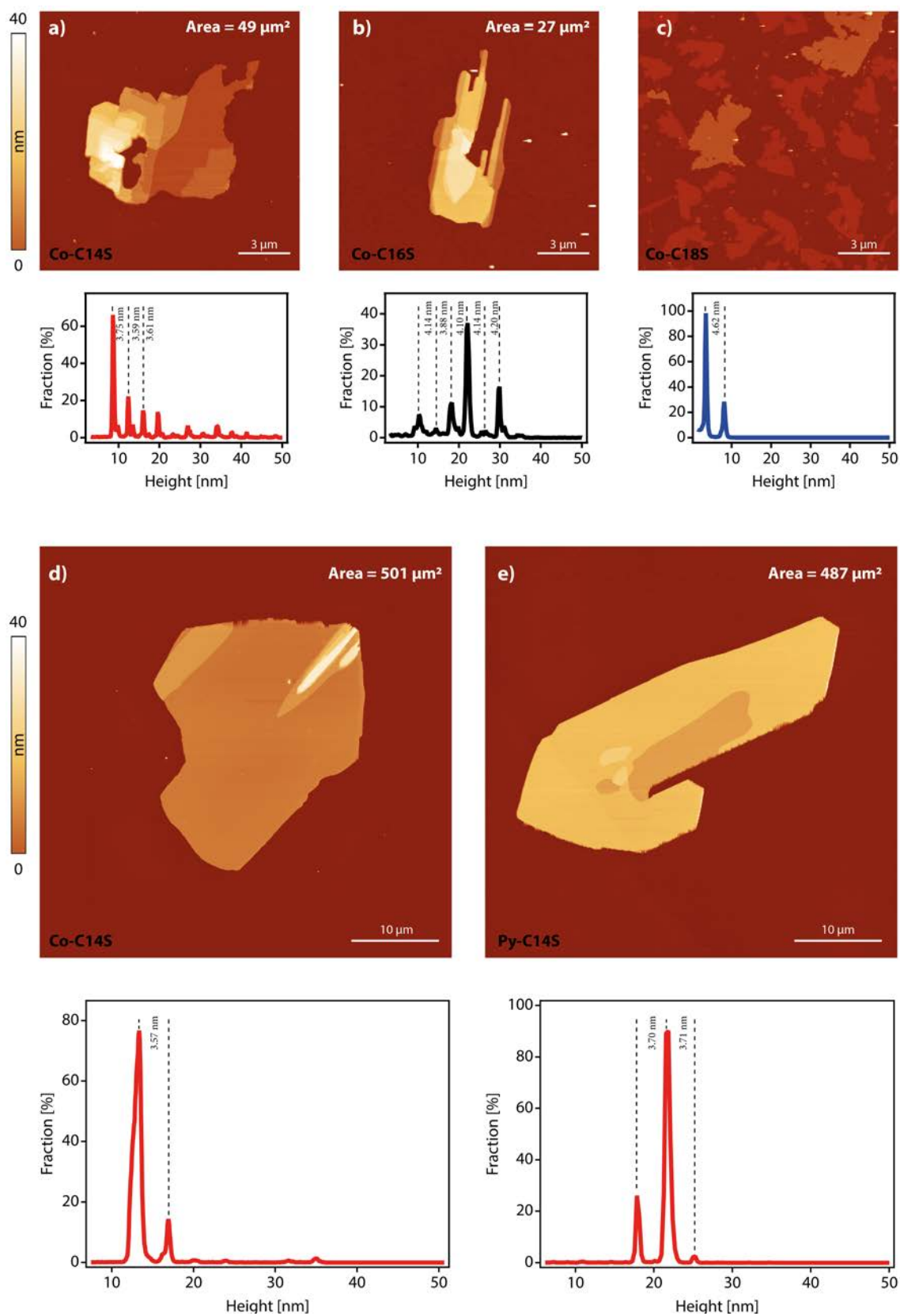
**Figure S2** – A C14S islands on Co imaged with different techniques: a) Optical image. b) Zoomed optical image with the contrast enhanced of the area marked by a red rectangle in a. c) SEM image of the area marked by a red rectangle in a. d) AFM images of the area marked by a black square in a. The number of layers (L) has been indicated next to each domain. 1L = 3.6 nm.



Supporting Information

**Figure S3** – A C14S island on Py imaged with different techniques a) AFM. b) Optical microscopy. c) Optical microscopy with a ND filter and d) SEM.



**Figure S4** - AFM topographic images and height distribution profiles of islands obtained with Co-C14S (a and d), Co-C16S (b), Co-C18S (c) and Py-C14 (e).

**Table S2** – Island Step height (ISH) and island average step height (IASH) estimated from AFM and XRD measurements and predicted for a SAM with its alkyl chain fully stretched. The XRD step heights have been calculated as two times the interlayer spacing determined from XRD measurements.

<b>Material</b>	<b>AFM [nm]</b>	<b>XRD [nm]</b>	<b>IASH [nm]</b>	<b>Predicted [nm]</b>
<b>M-C14S</b>	3.6	3.5	3.6	1.8
<b>M-C16S</b>	4.1	4.2	4.1	2.0
<b>M-C18S</b>	4.5	4.6	4.6	2.3

**Table S3** - Statistical parameters obtained from histograms in Figure 4: Island Average Height (IAH), Most Probable Height MPH, P85 and P50. P85(50) represents the height below which 85(50)% of the observations fall.

<b>Material</b>	<b>IAH [nm]</b>	<b>MPH [nm]</b>	<b>P50 [nm]</b>	<b>Number of layers<sup>a</sup></b>	<b>P85 [nm]</b>	<b>Number of layers<sup>a</sup></b>
<b>Co-C14S</b>	14.9	10.8	9.9	3	18.1	5
<b>Co-C16S</b>	14.7	8.2	7.5	2	16.0	4
<b>Co-C18S</b>	3.2	5.5	2.7	1	4.6	1
<b>Py-C14S</b>	30.2	29.8	27.7	8	41.0	11
<b>Py-C16S</b>	14.2	8.2	7.4	2	24.0	6
<b>Py-C18S</b>	7.1	3.6	3.4	1	8.2	2

<sup>a</sup>Number of layer values are calculated from P50 and P85 considering that a single layer thickness, that is, the island average step height (IASH): is 3.6, 4.1 and 4.6 nm for C14S, C16S and C18S, respectively.

**Table S4** -  $d_{\text{CH}_2}$ ,  $2d_0$  and tilt angel (TA) values obtained from our AFM and XRD data compared with values obtained from the literature for bulk LMAs.

<b>Material</b>	<b><math>2d_{\text{CH}_2}</math>[nm]</b>	<b><math>2d_0</math>[nm]</b>	<b>TA [°]</b>	<b>Ref.</b>	<b>Compound</b>
<b>Ni</b>	0.258	0.78	0	1	Ni(SR) <sub>2</sub>
<b>Pd</b>	0.248	0.81	7	2	Pd(SR) <sub>2</sub>
<b>Ag</b>	0.248	0.98	7	2	AgSR
<b>Ag</b>	0.250	0.97	0	3	AgSR
<b>Ag</b>	0.241	1.02	15	4	AgSR
<b>Ag</b>	0.242	1.05	15	5-7	AgSR
<b>Py/Co (AFM)</b>	0.225	0.92	26	This work	
<b>Co (XRD)</b>	0.215	1.05	31	This work	

**Figure S5** - Representative 100x optic images of Co and Py functionalized samples.

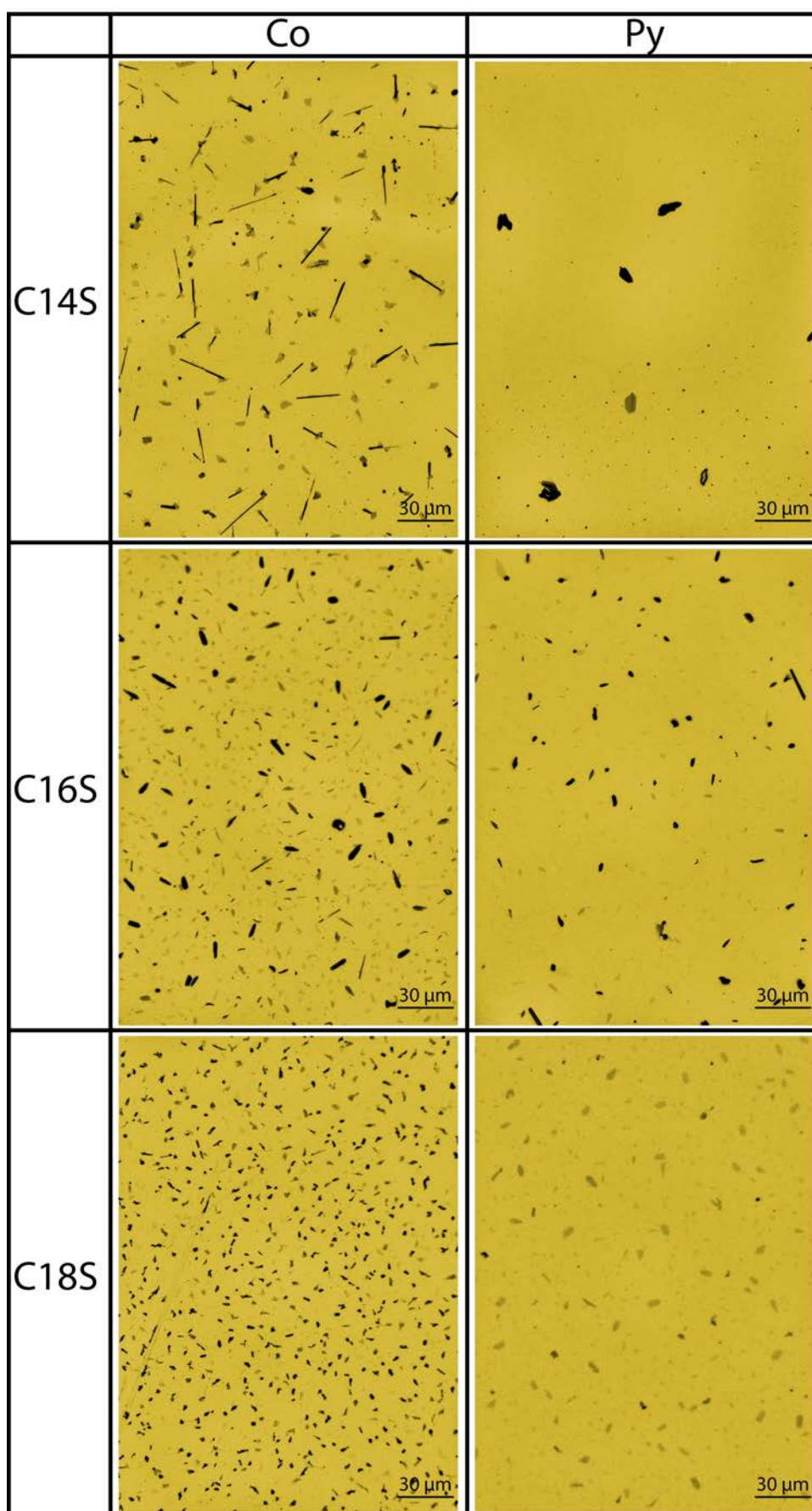


**Table S5** - Statistical parameters obtained from histograms in Figure 4: Island Average Area (IAA), Most Probable Area (MPA), Number of Island (N), P85, P50 and total coverage (C). P85(50) represents the area below which 85(50)% of the observations fall.

Material	IAA [ $\mu\text{m}^2$ ]	MPA [ $\mu\text{m}^2$ ]	P50 [ $\mu\text{m}^2$ ]	P85 [ $\mu\text{m}^2$ ]	C [%]	$\text{Na} / 10^4$ $\mu\text{m}^2$
Co-C14S	53.3	30	39.3	85.8	5	12
Co-C16S	8.4	15	13.9	24.5	7	54
Co-C18S	7.5	5	3.7	8.8	18	483
Py-C14S	39.7	5	15.5	85.1	1	8
Py-C16S	9.7	5	6.3	12.3	3	51
Py-C18S	9.9	5	4.6	11.6	5	112

<sup>a</sup>Estimated as  $C = \text{P50} / C$

**Figure S6** – Coverage dependence as a function of the LMA chain length.

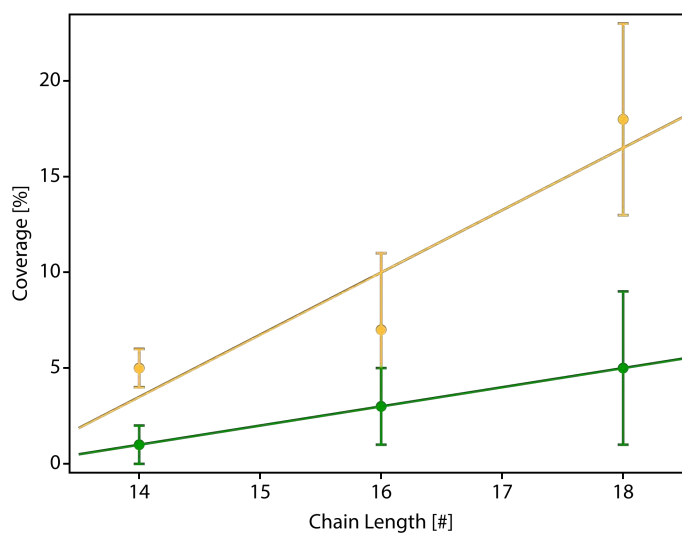


**Figure S7** - Real time growth of C18S-Co island domains, imaged with AFM.

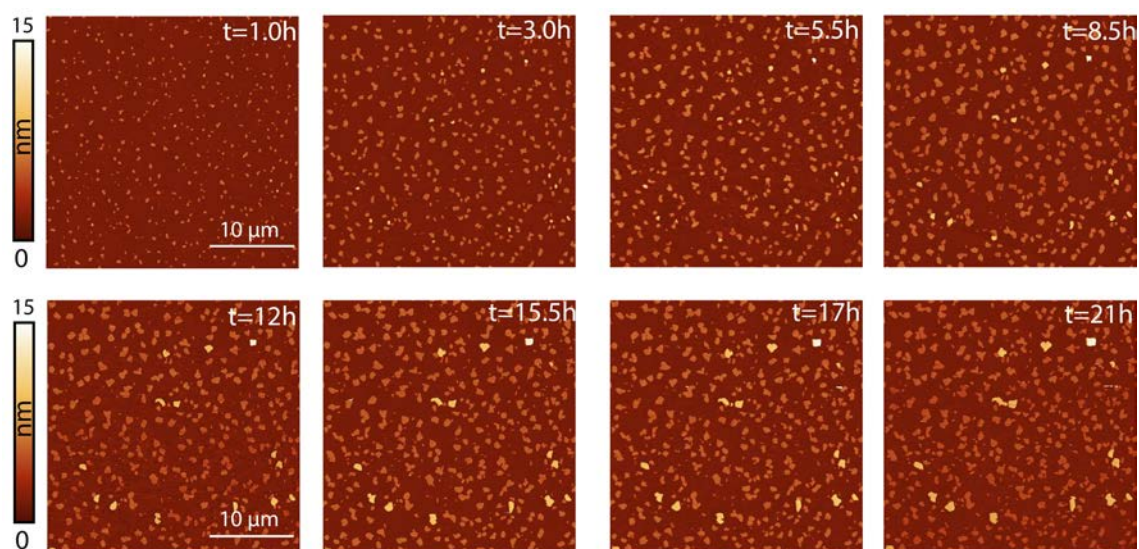


**Figure S8** - Real time growth of C14S-Co island domains, imaged with AFM.

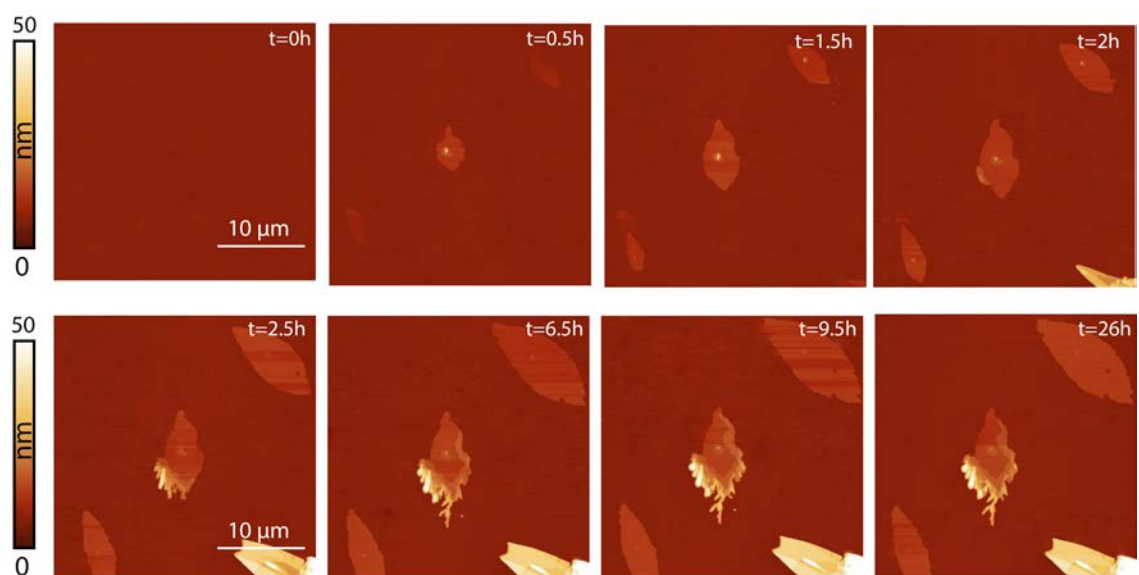


**Figure S9** - Optical images of a Co-C14S sample exposed to air for 0 to 35 minutes.

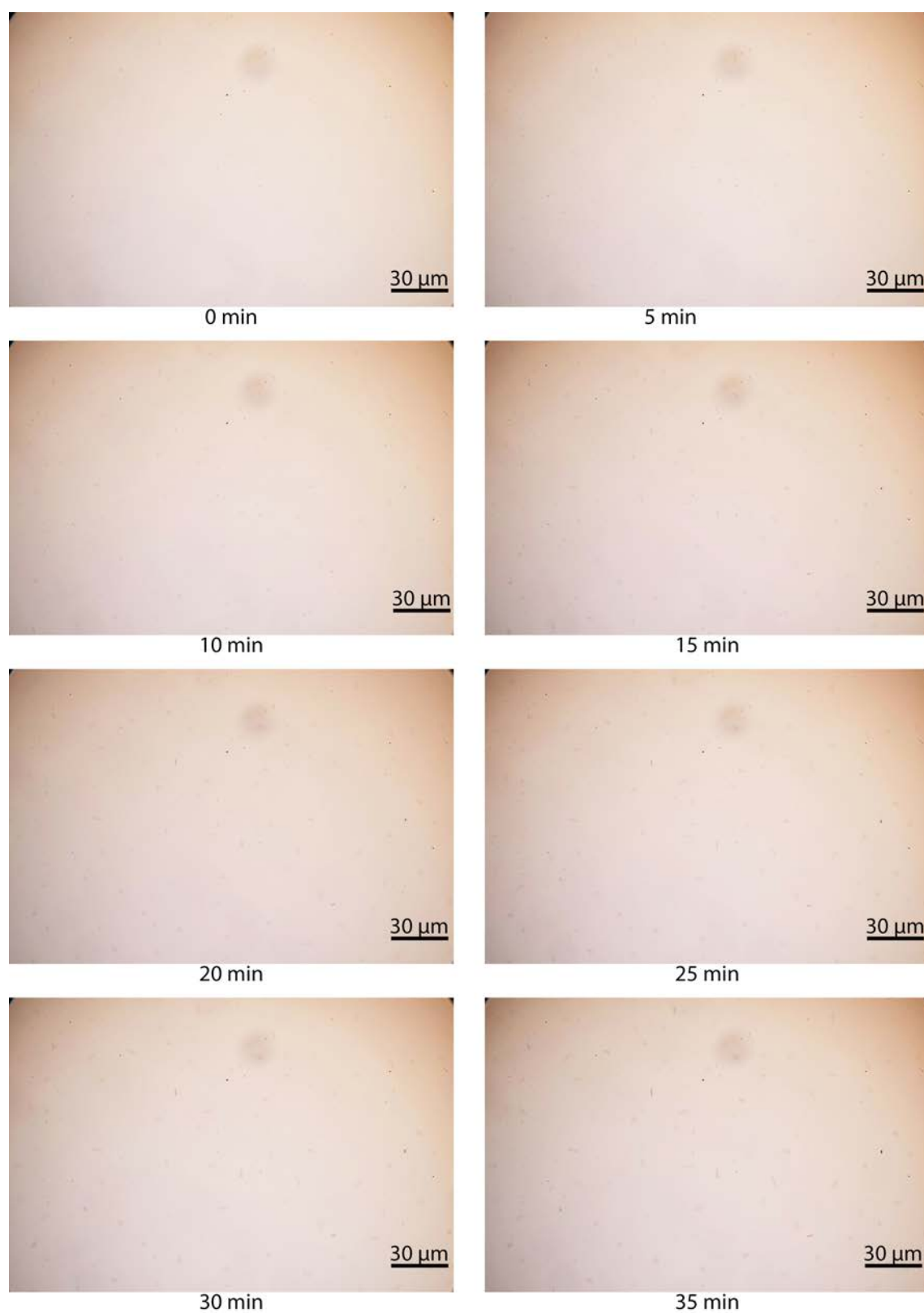


**Figure S10** - Optical images of a Co-C14S sample exposed to air for 40 to 75 minutes

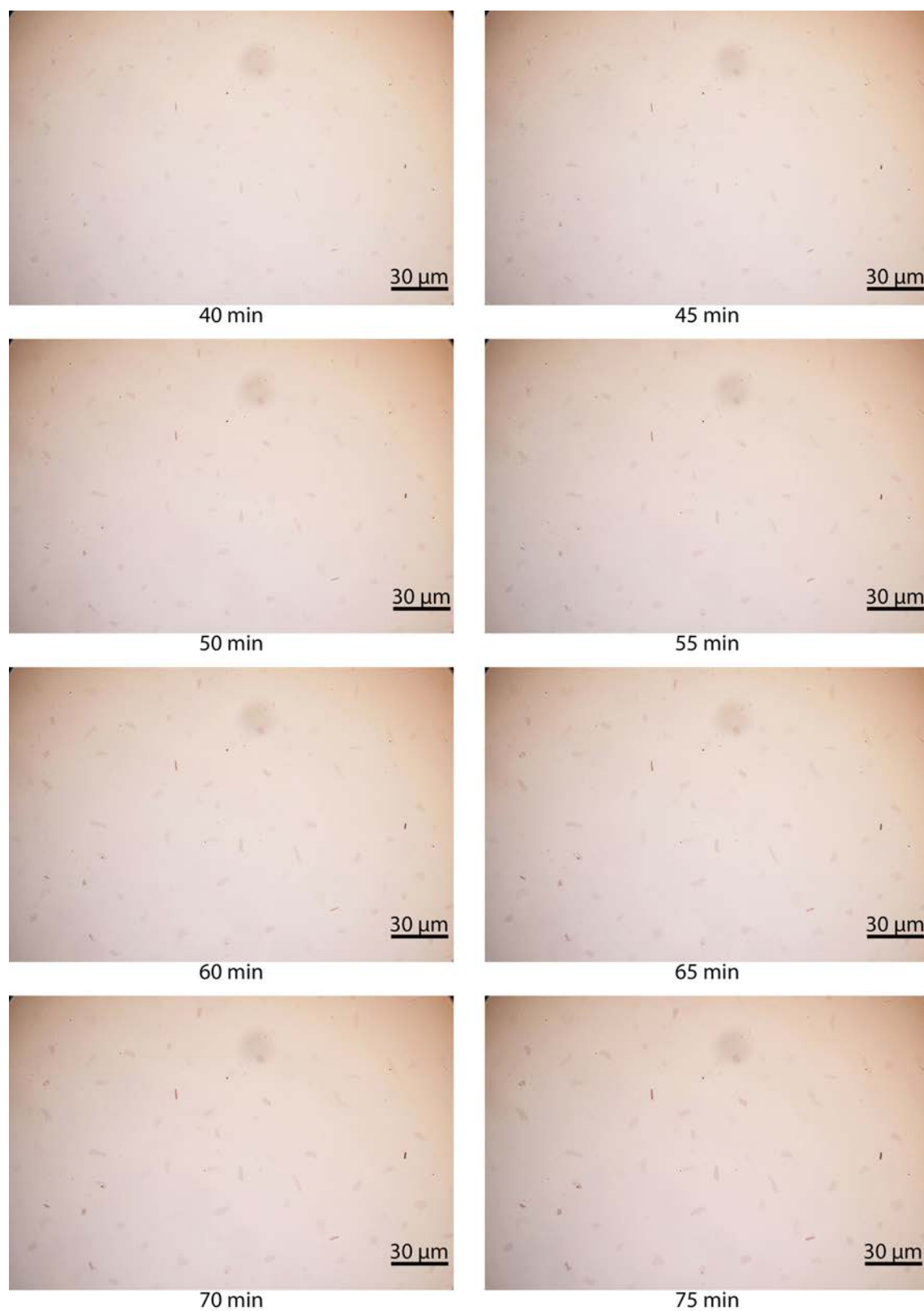


**Figure S11** - Optical images of a Co-C14S sample exposed to air for 80 to 115 minutes.

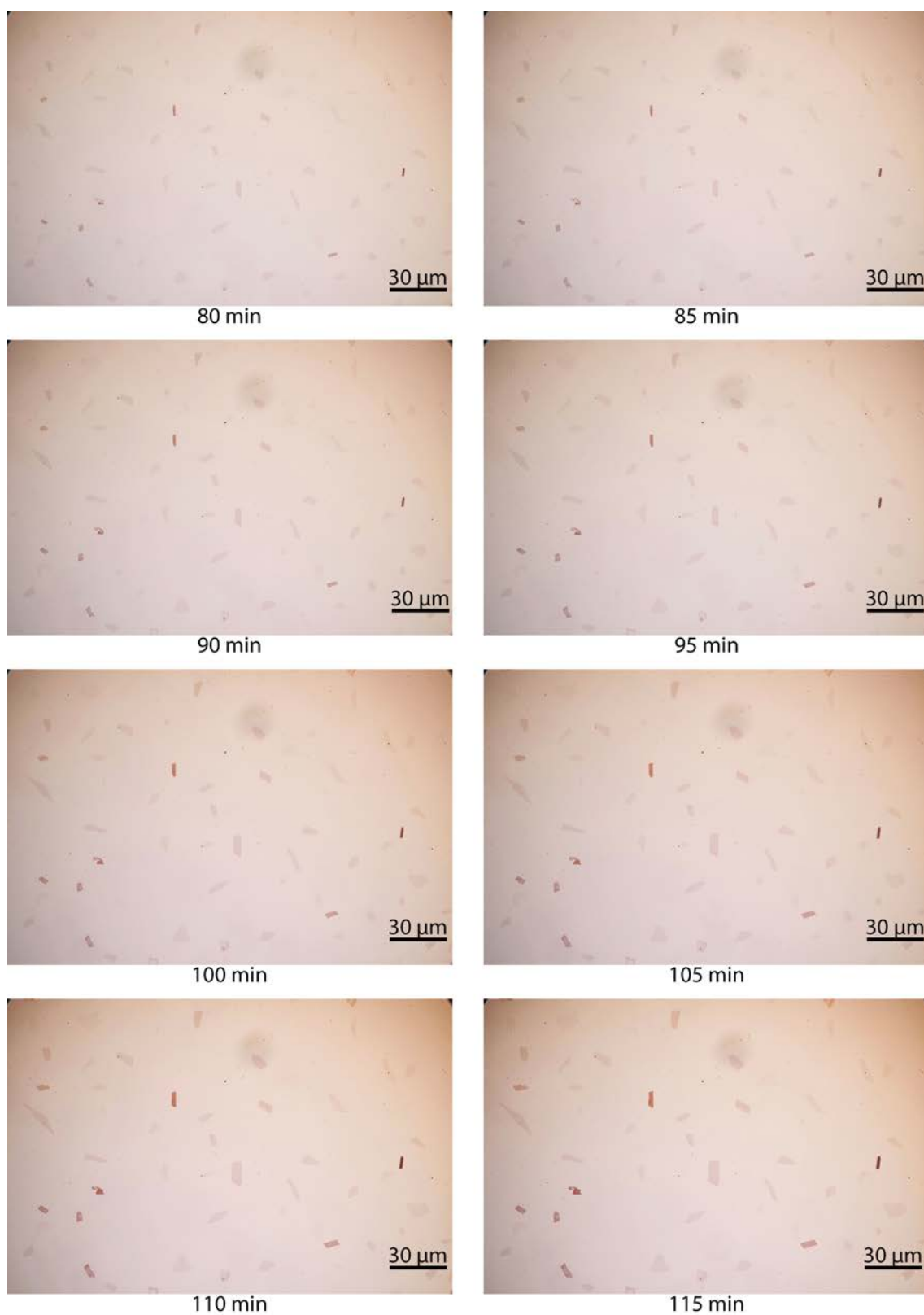


**Figure S12** - Optical images of a Co-C14S sample exposed to air for 120 to 1980 minutes.

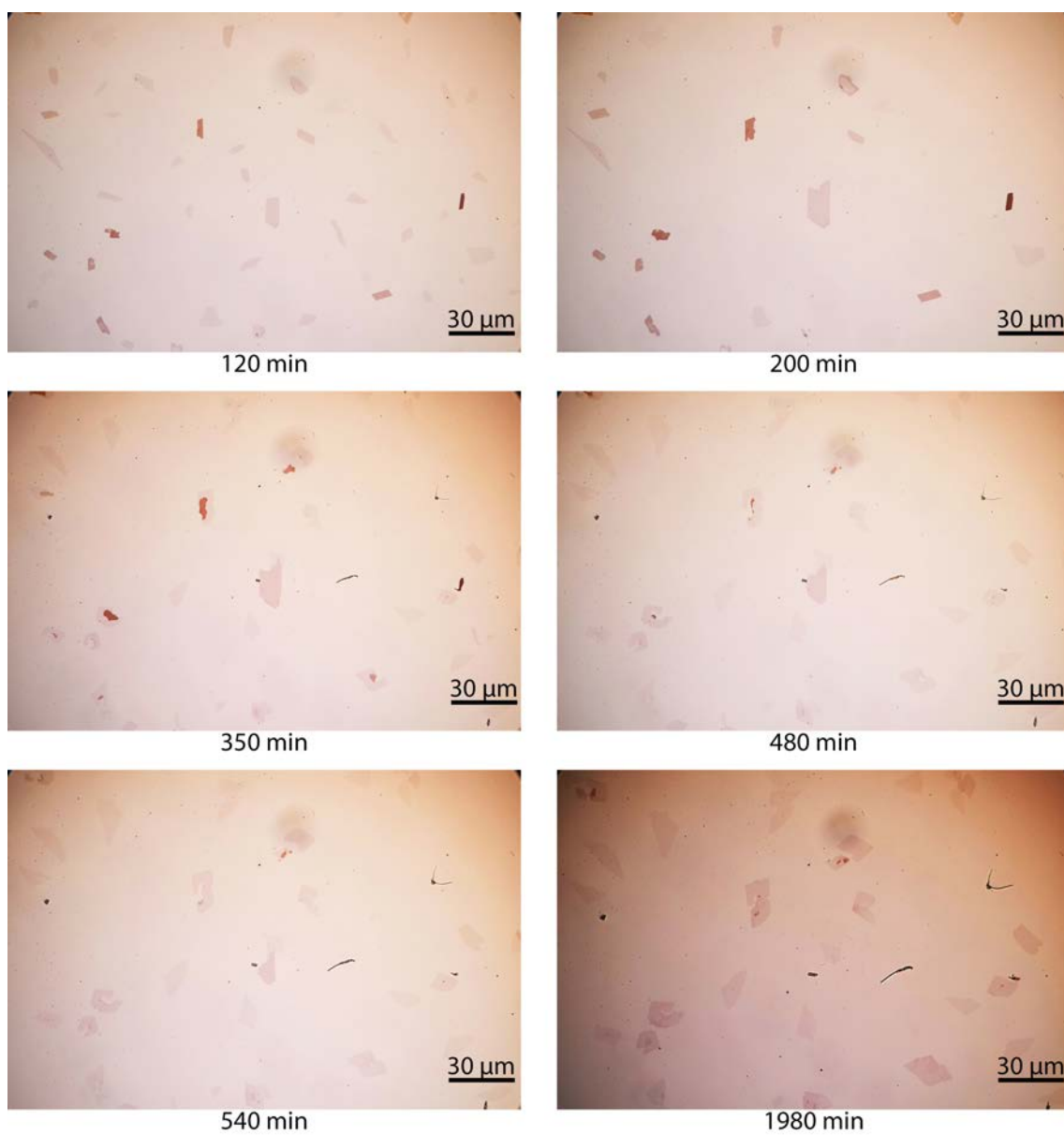


**Figure S13** - Optical images of a Co-C14S samples exposed to the air at different temperatures for 23 hours, with their correspondent area distribution histograms and histogram area integrals (yellow dashed line).

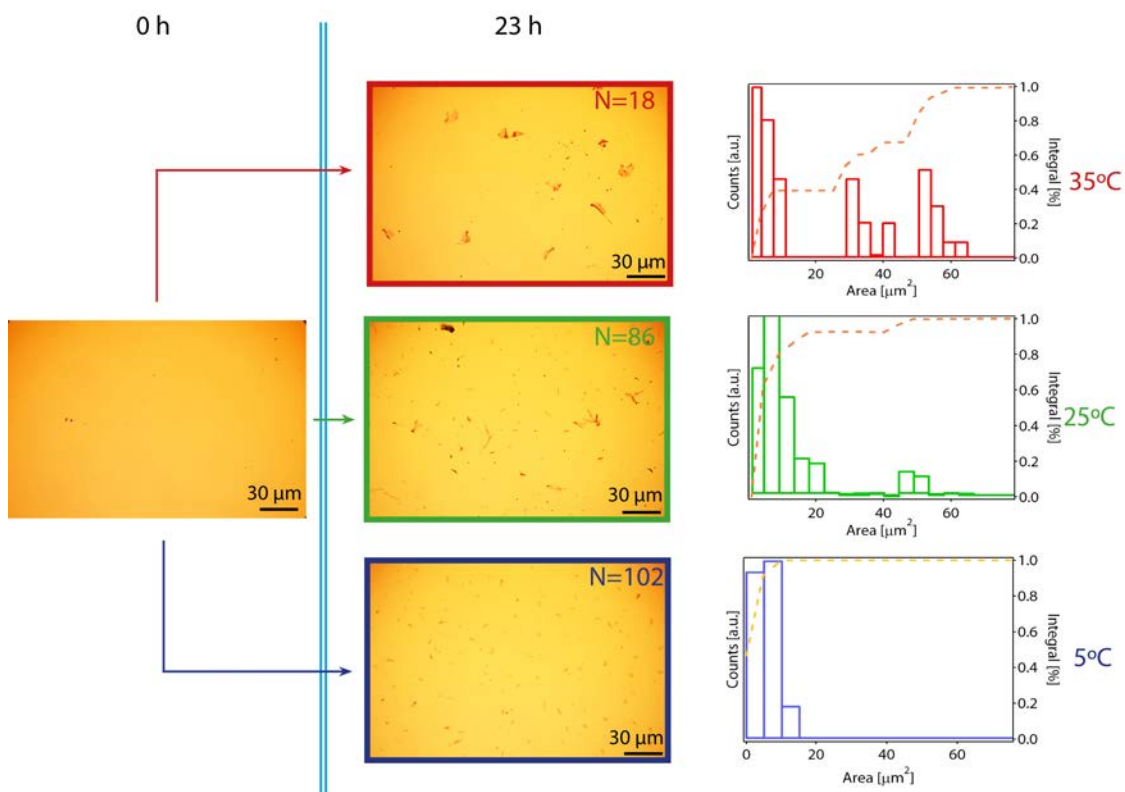


**Figure S14** - Optical images of Co-C14S substrates after 16h of exposure to air (or dry air) and additional 16 h in air (32h).

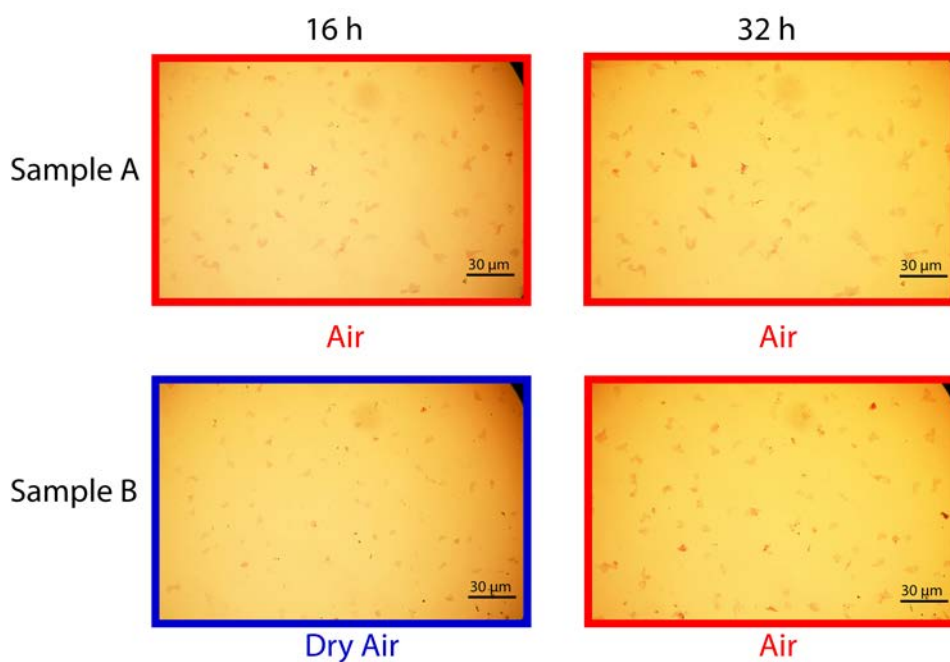
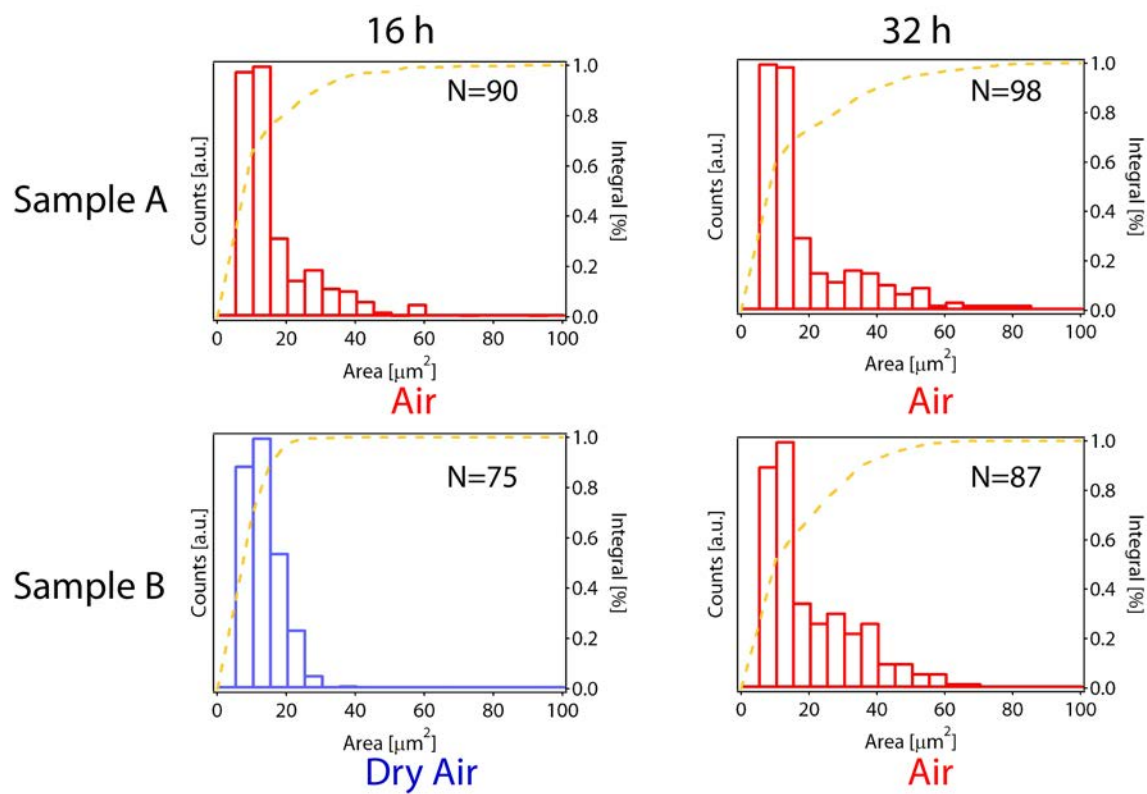


**Figure S15** - Area distribution from the samples displayed in Figure S14 after 16h in air (or dry air) and additional 16 h in air. Yellow dashed line represents the histogram integrals. N is the number of islands in the image.



**References:**

- [1] N.S. John, G.U. Kulkarni, A. Datta, S.K. Pati, F. Komori, G. Kavitha, et al., *Magnetic Interactions in Layered Nickel Alkanethiolates*, **J. Phys. Chem. C** 111 (2007) 1868–1870.
- [2] F. Bensebaa, T.H. Ellis, E. Kruus, R. Voicu, Y. Zhou, *Characterization of Self-Assembled Bilayers: Silver–Alkanethiolates*, **Langmuir** 14 (1998) 6579–6587.
- [3] A.N. Parikh, S.D. Gillmor, J.D. Beers, K.M. Beardmore, R.W. Cutts, B.I. Swanson, *Characterization of Chain Molecular Assemblies in Long-Chain, Layered Silver Thioliates: A Joint Infrared Spectroscopy and X-ray Diffraction Study*, **J. Phys. Chem. B** 103 (1999) 2850–2861.
- [4] I.G. Dance, K.J. Fisher, R. Banda, *Layered structure of crystalline compounds silver thioliates (AgSR)*, **Inorg. Chem.** 30 (1991) 183–187.
- [5] L. Hu, Z. Zhang, M. Zhang, M.Y. Efremov, E.A. Olson, L.P. de la Rama, et al., *Self-Assembly and Ripening of Polymeric Silver–Alkanethiolate Crystals on Inert Surfaces*, **Langmuir** 25 (2009) 9585–9595.
- [6] L. Hu, L.P. de la Rama, M.Y. Efremov, Y. Anahory, F. Schiettekatte, L.H. Allen, *Synthesis and Characterization of Single-Layer Silver–Decanethiolate Lamellar Crystals*, **J. Am. Chem. Soc.** 133 (2011) 4367–4376.
- [7] Z. Ye, L.P. de la Rama, M.Y. Efremov, J.-M. Zuo, L.H. Allen, *Approaching the size limit of organometallic layers: synthesis and characterization of highly ordered silver–thiolate lamellae with ultra-short chain lengths*, **Dalton Trans.** 45 (2016) 18954–18966.